

Literature Report

Reporter: 许宁

Date: 2020-7-16

Article

Visible light mediated bidirectional control over carbonic anhydrase activity in cells and *in vivo* using azobenzene sulfonamides

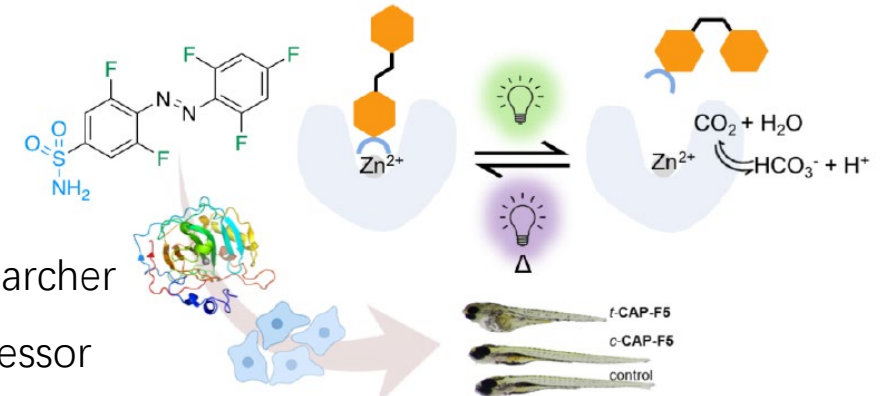
Kanchan Aggarwal, Timothy P. Kuka, Mandira Banik, Brenda P. Medellin, Chinh Q. Ngo, Da Xie, Yohaan Fernandes, Tyler L. Dangerfield, Elva Ye, Bailey Bouley, Kenneth A Johnson, Yan Jessie Zhang, Johann K. Eberhart, and Emily L. Que

J. Am. Chem. Soc., Just Accepted Manuscript • DOI: 10.1021/jacs.0c05383 • Publication Date (Web): 04 Jul 2020



Assistant Prof. Emily L. Que, Ph.D.

- 2000-2004 University of Minnesota, BS
2004-2009 University of California, Berkeley PhD
2009-2014 Northwestern University Post-doctoral researcher
2014- University of Texas, Austin Assistant Professor



Research interest:

1. The development of chemical tools to probe cellular metal homeostasis
2. The development of novel MRI contrast agents for molecular imaging



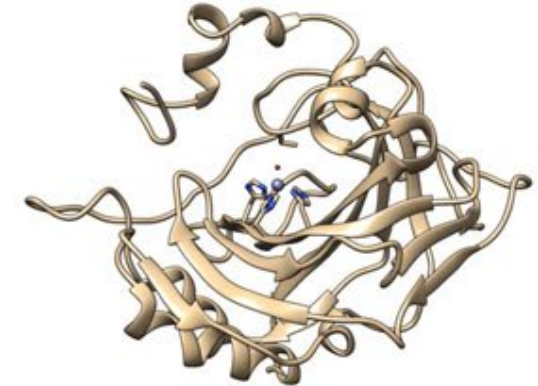
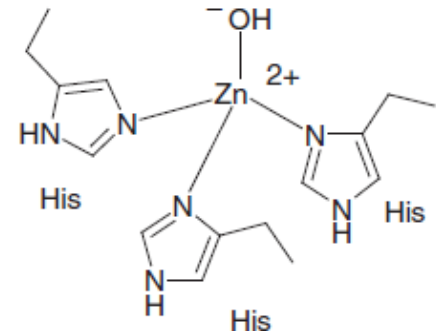
Carbonic anhydrases

Carbonic anhydrases (CA) since 1933

α -CA	β -CA	γ -CA	δ -CA	ζ -CA	η -CA
绿色植物和革兰氏阴性细菌、原生动物、藻类、脊椎动物、高等植物、阳性细菌、古生菌、海洋硅藻、海洋硅藻、原生动物	高等植物、革兰氏阴性和真菌、藻类、大多数细菌	古生菌、蓝藻和大多数细菌	海洋硅藻	海洋硅藻	原生动物

人类CA (α 类) 15种不同的亚型。其中12个异构体存在活性位点，使其具有催化活性 (CAs I–IV, CAs VA–VB, CAs VI–VII, CA IX和CA XII–XIV)。而异构体CA VIII, X 和XI没有催化活性，被称为CA相关蛋白 (CA-RP)。

其中，CA IX和CA XII 被视为抗癌靶标，其中CA IX特别受关注，因为它在实体瘤中高表达而在正常组织中却低表达。



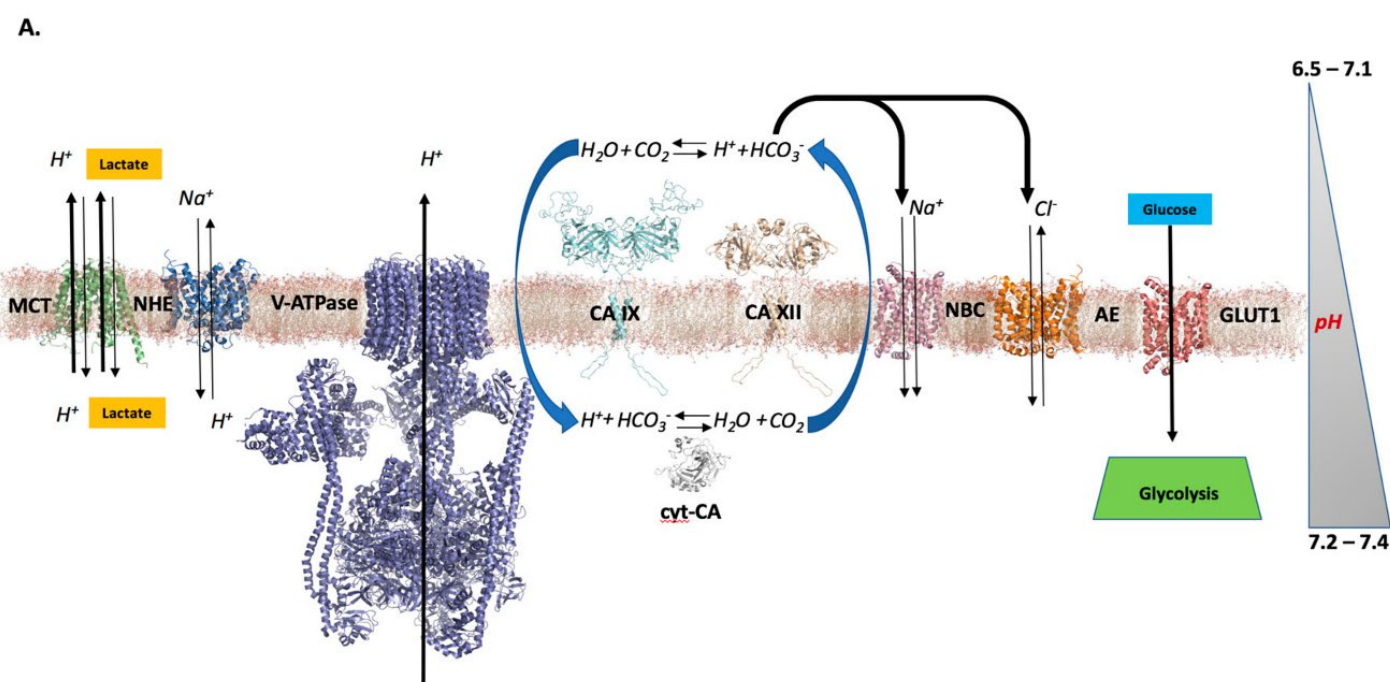
大多数CAs的活性部位含有一个锌离子、三个组氨酸残基和一个水分子

Reactions catalysed by CAs

$O=C=O + H_2O \rightleftharpoons HCO_3^- + H^+$	(1)
$O=C=S + H_2O \rightleftharpoons H_2S + CO_2$	(2)
$S=C=S + 2H_2O \rightleftharpoons 2 H_2S + CO_2$	(3)
$HN=C=NH + H_2O \rightleftharpoons H_2NCONH_2$	(4)
$RCHO + H_2O \rightleftharpoons RCH(OH)_2$	(5)
$RCOOAr + H_2O \rightleftharpoons RCOOH + ArOH$	(6)
$RSO_3Ar + H_2O \rightleftharpoons RSO_3H + ArOH$	(7)
$ArOP_3H_2 + H_2O \rightleftharpoons ArOH + H_3PO_4$	(8)
$R_2NCSSR' + H_2O \rightleftharpoons R_2NH + R'SH + COS$	(9)
$PhCH_2OCOCl + H_2O \rightleftharpoons PhCH_2OH + CO_2 + HCl$	(10)
$RSO_2Cl + H_2O \rightleftharpoons RSO_3H + HCl$	(11)

How CA activity can regulate and foster the unique pH differential within a tumor cell ?

大多数正常细胞, $pH_i = 7.2$, $pHe \geq 7.3$ 。



B.

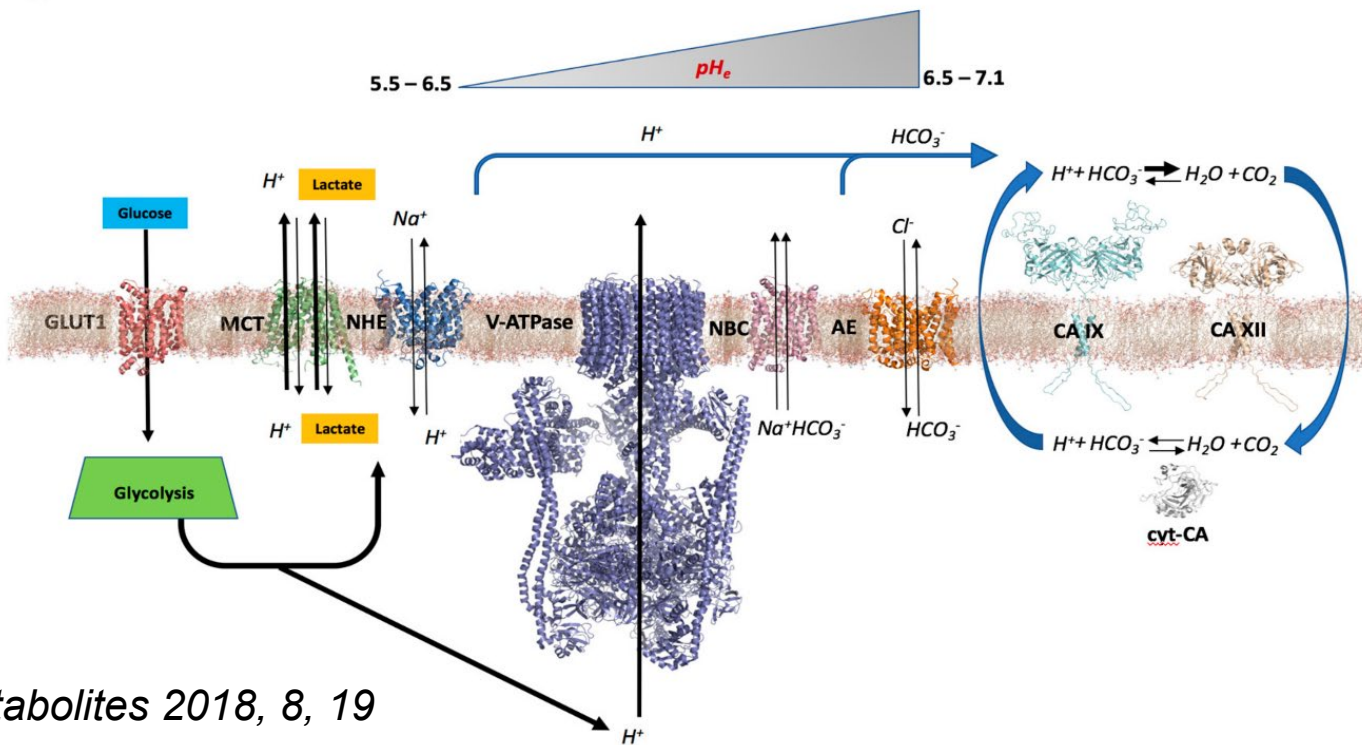
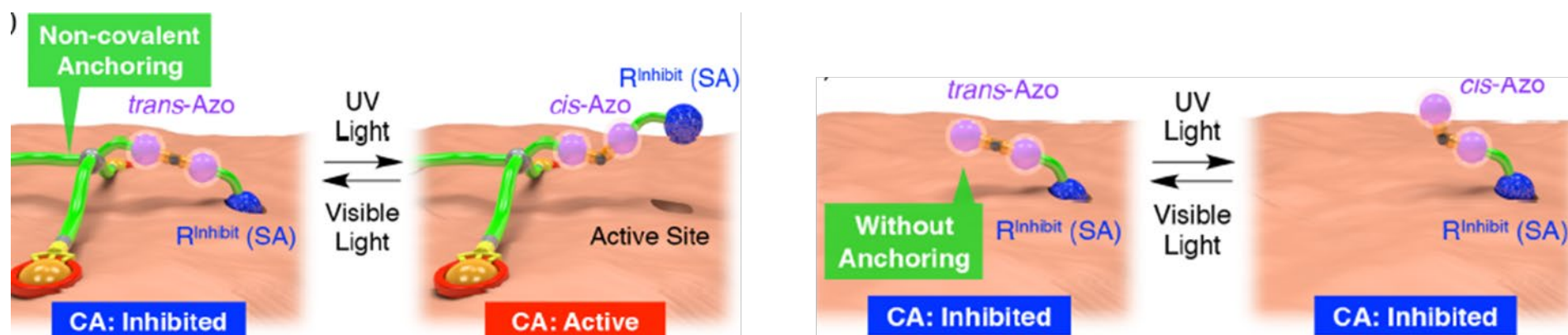
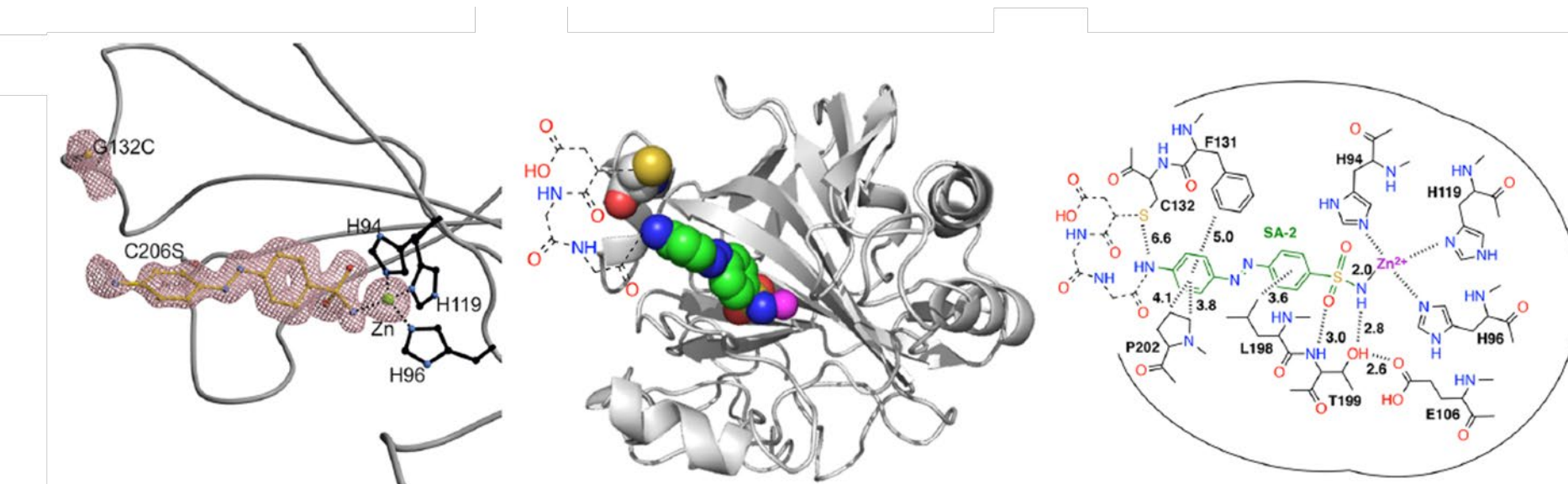


Fig. Illustrations of Hypothesis 1 (A) and Hypothesis 2 (B) to model the functional role of CA in the hypoxic tumor microenvironment.

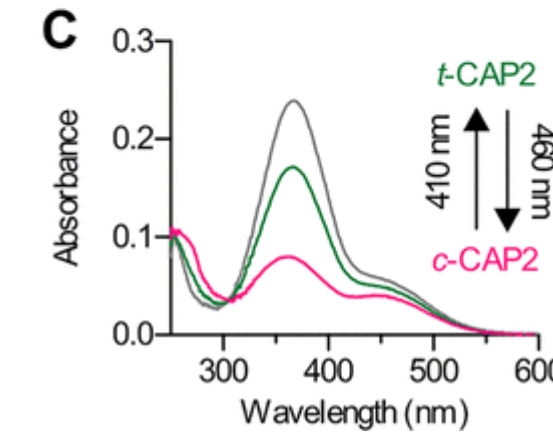
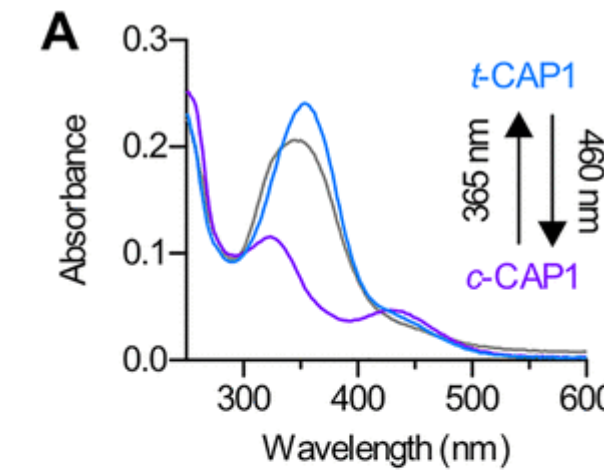
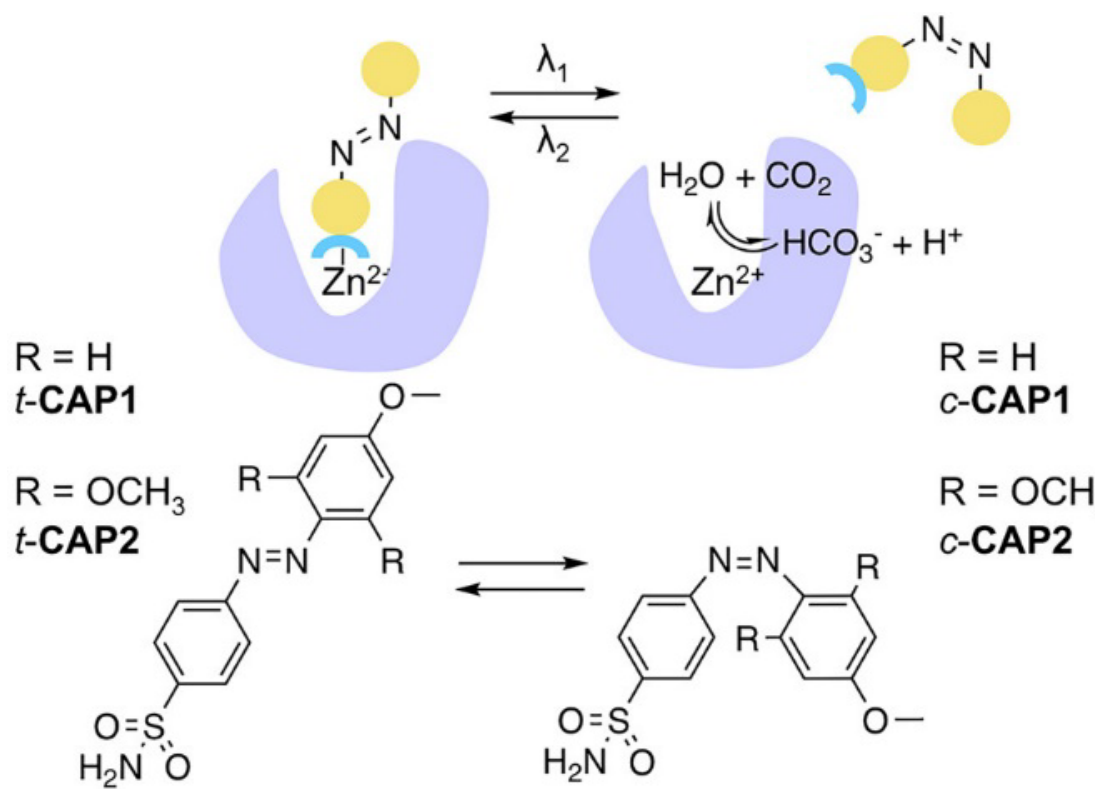


Azobenzene-based photoswitches for CA





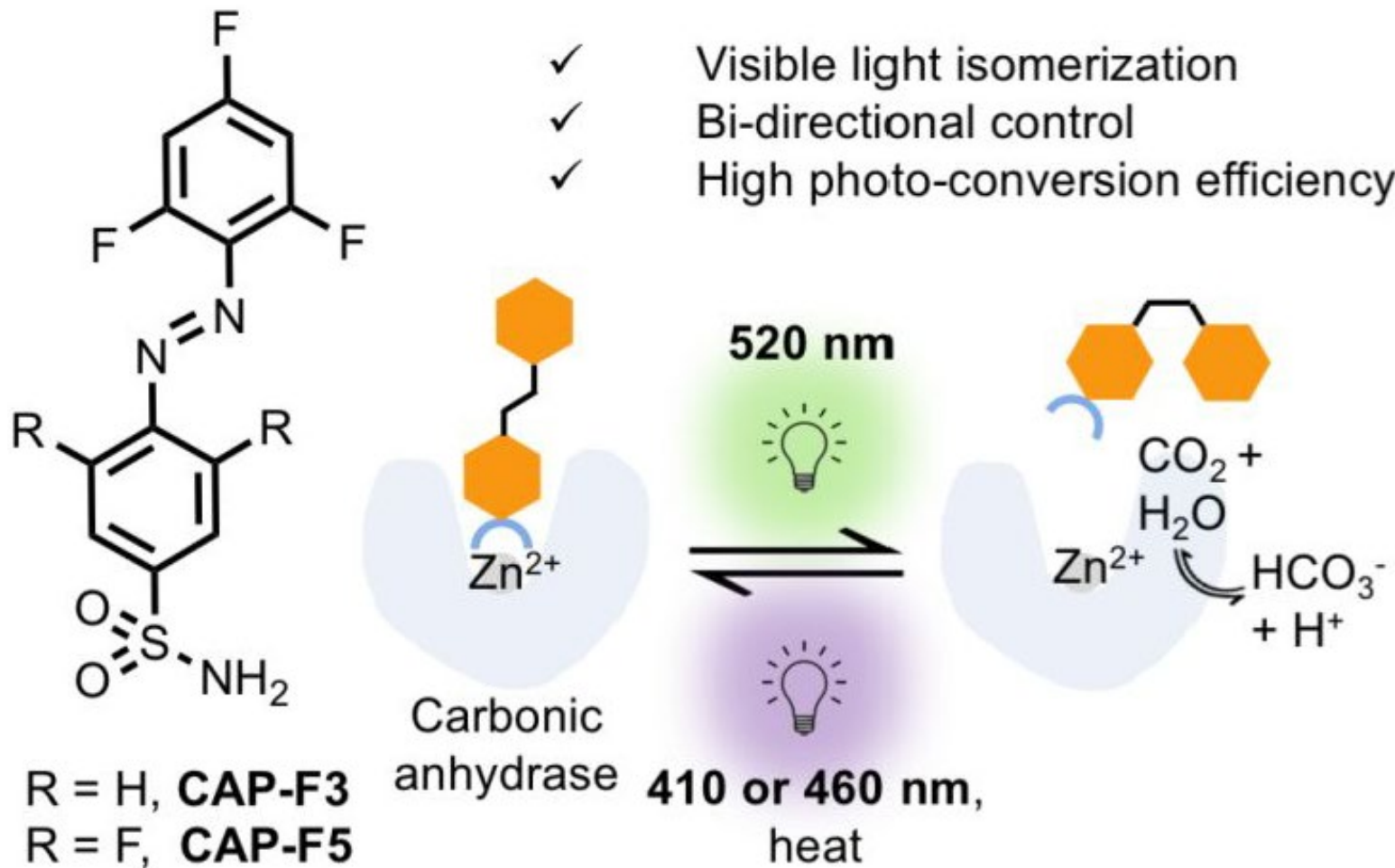
In Situ Photoregulation of Carbonic Anhydrase Activity



紫外光进行光异构化
光转化效率低
顺式异构体热稳定性差



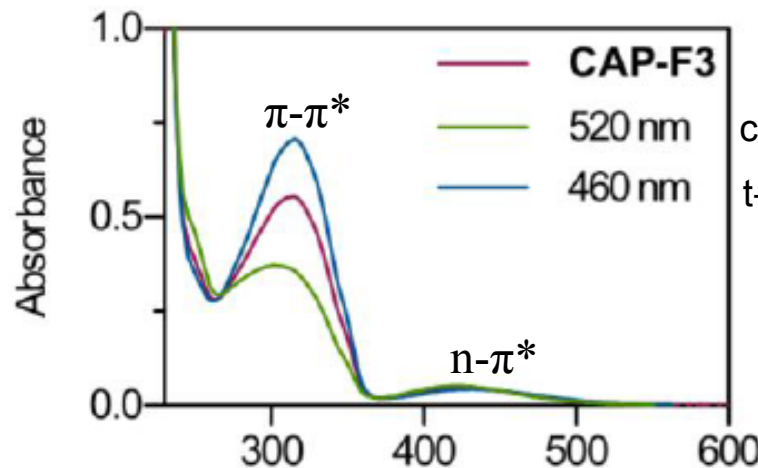
Structures of CAP-F3 and CAP-F5



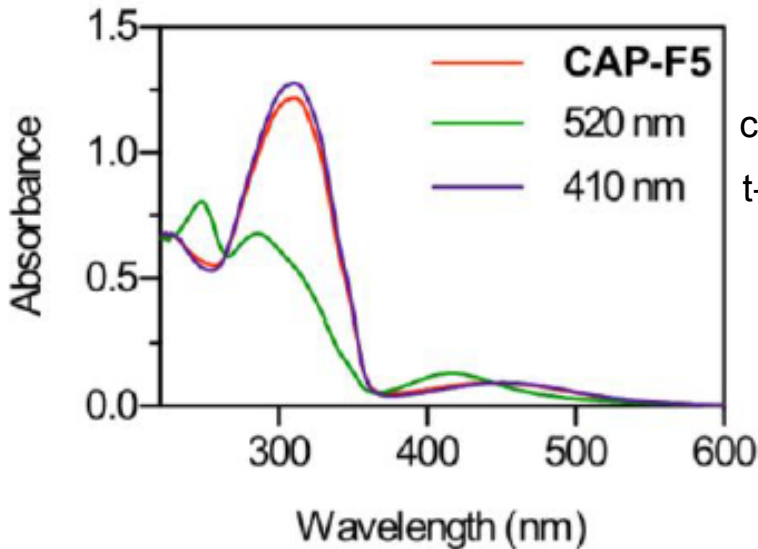
Scheme 1. Structures of CAP-F3 and CAP-F5, and photoswitching in the presence of carbonic anhydrase.



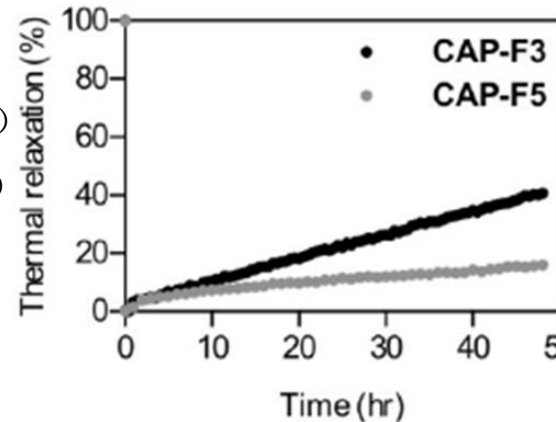
Photoisomerization efficiency and Thermal stability

A

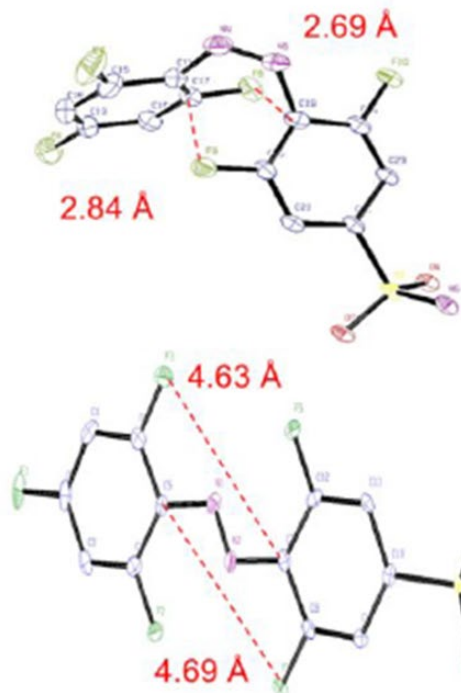
c-CAP-F3 (71%)
t-CAP-F3 (58%)

B

c-CAP-F5 (87%)
t-CAP-F5 (82%)



c-CAP-F5 \rightarrow t-CAP-F5 约为 15%
c-CAP-F3 \rightarrow t-CAP-F3 约为 40%



C-F键的范德瓦尔斯距离 (3.17 Å)

顺式异构体中存在C••F相互作用

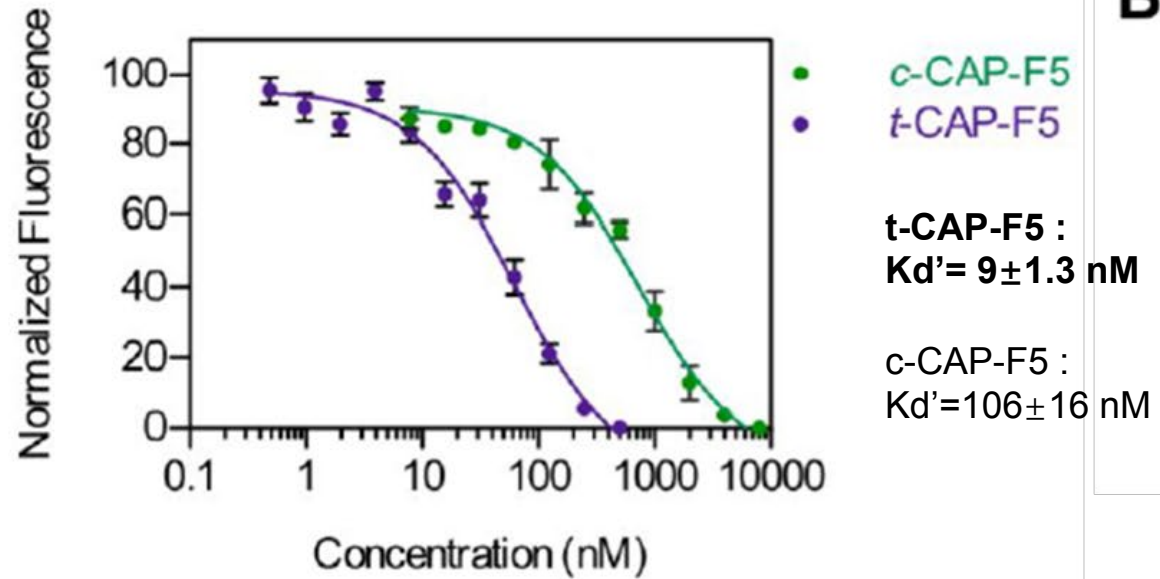
Figure 1. UV-vis spectra of CAP-F3 (A) and CAP-F5 (B) before and after photoradiation (cis 520 nm for 5 minutes; trans 460/410 nm for 2 min).

Figure 2. Thermal relaxation of c-CAP-F3 and c-CAP-F5 in aqueous buffer at 37°C. Single crystal structure of c-CAP-F5 and t-CAP-F5.

The difference in binding preference between c-CAP-F5 and t-CAP-F5 towards CA

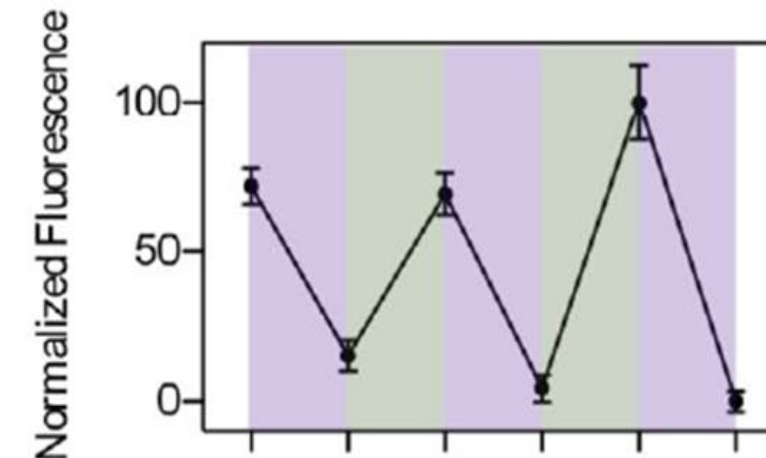
用t-CAP-F5和c-CAP-F5滴定bCA•DNSA溶液，计算表观Kd值。

A

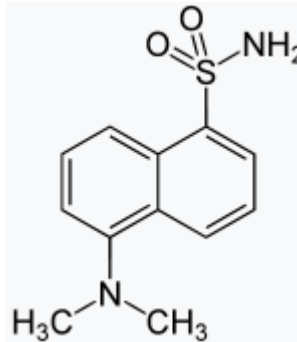


B

$Kd' = 1.6 \mu M$



410nm照射后，DNSA的荧光强度降低，
520nm照射后荧光强度增加。



Dansylamide：一种基于磺胺的CA抑制剂

当与CA的活性部位结合时，其在458nm处的荧光增强，当外部配体将其从活性部位移开时，其荧光减弱。

Figure 3. (A) Change in fluorescence emission ($\lambda_{ex} = 280 \text{ nm}$; $\lambda_{em} = 458 \text{ nm}$) of bCA-DNSA mixture in the presence of different concentrations of t-CAP-F5 and c-CAP-F5 to determine apparent Kd values. (B) The binding of CAP-F5 is reversible in nature as shown by irradiating the sample of CA, **DNSA** and probe with alternate 520 nm and 410 nm for in situ isomerization and monitoring DNSA fluorescence.

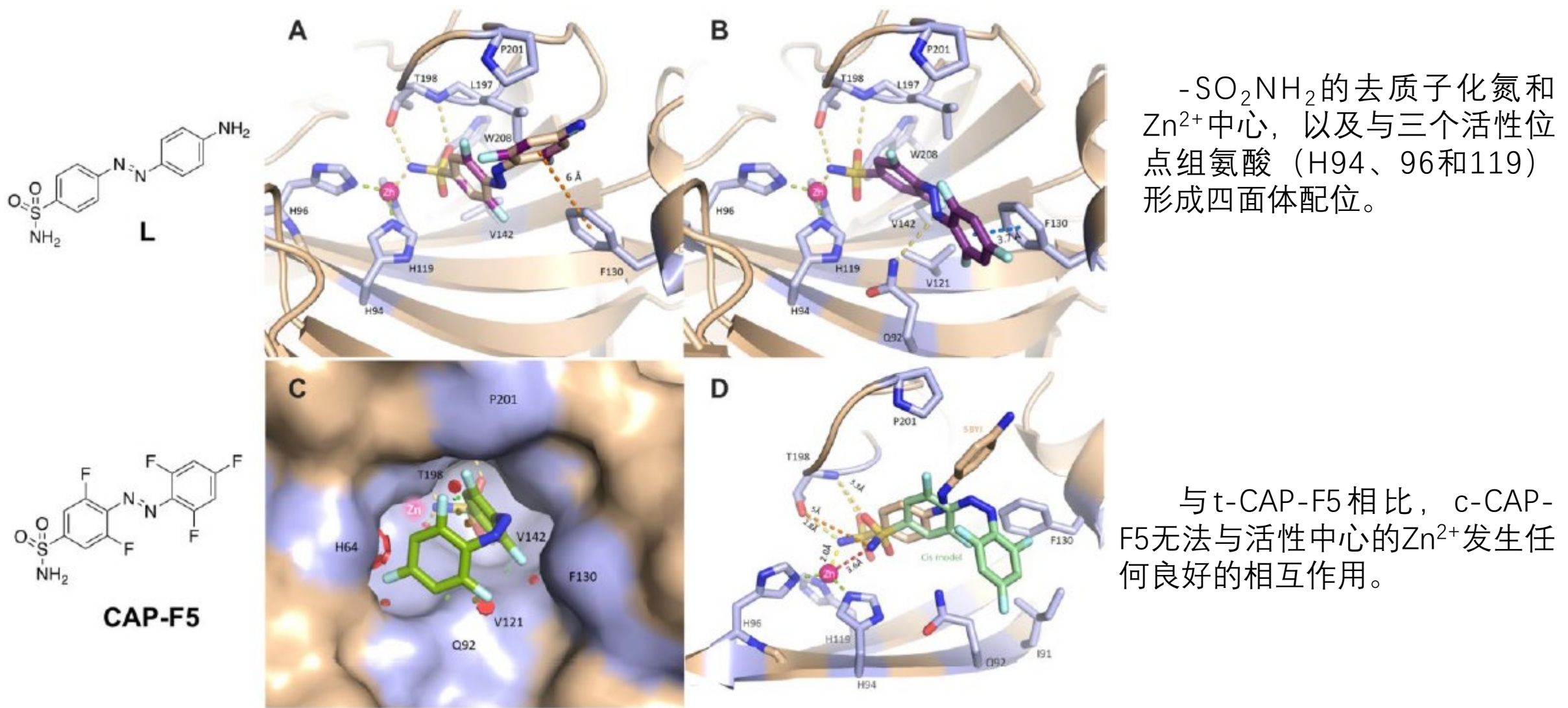
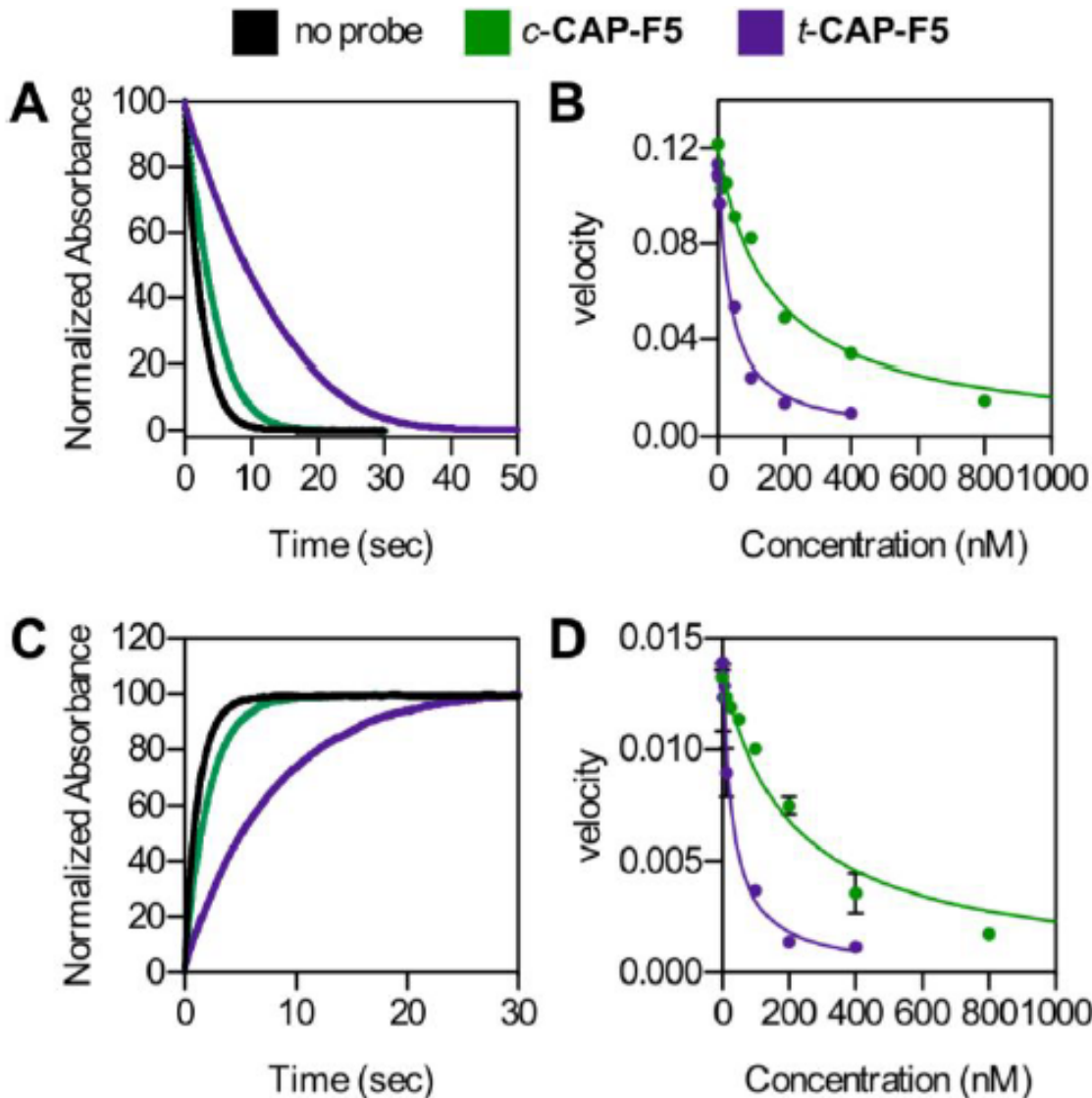


Figure 4. Docking of CAP-F5 in the active site of hCAII structure obtained with azobenzene ligand L bound to the active site (PDB 5BYI). The secondary Protein (PDB 5BYI) is shown with side chains of active site residues in sticks. (A) Docking of t-CAP-F5 into the hCAII active site after superimposing it onto the ligand L. (B) Alternative binding mode for t-CAP-F5 due to the presence of fluorine atoms. (C) Docking of c-CAP-F5 when interactions between $-\text{SO}_2\text{NH}_2$ and Zn^{2+} are kept intact, steric clashes are shown as red disks. (D). Potential orientation of c-CAP-F5 when steric clashes are removed, showing the probe retreats from the active site.

► Modulate both the CO₂ hydration and bicarbonate dehydration activity of CA.



以饱和CO₂水溶液为底物，在CAP-F5的反式和顺式异构体存在下，催化反应的初始速率分别为0.025s⁻¹和0.082s⁻¹。

以饱和KHCO₃水溶液为底物，在CAP-F5的反式和顺式异构体存在下，催化反应的初始速率分别为 0.36×10^{-2} s⁻¹和 1.0×10^{-2} s⁻¹

Figure 5. Change in absorbance of **phenol red** ($\lambda=557\text{nm}$) due to CO₂ hydration activity (A) and HCO₃⁻ dehydration activity (C) of CA in the absence and presence of 1eq of trans and cis CAP-F5; Change in CO₂ hydration (B) and HCO₃⁻ dehydration (D) catalytic velocity as a function of trans and cis isomer concentration.

► Applied CAP-F5 to control the activity of CA in cell culture

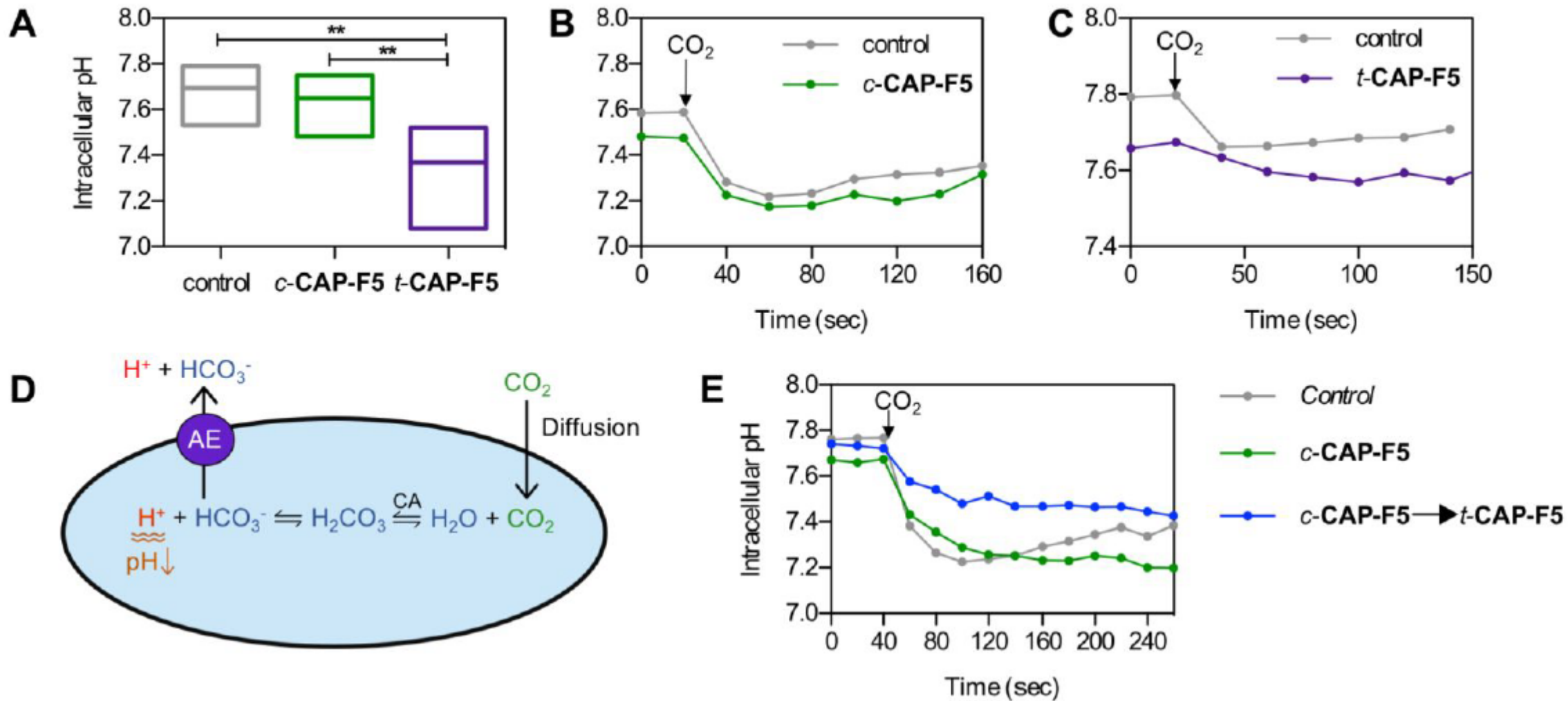


Figure 6. (A) The intracellular pH of HeLa cells as a result of incubation of t-CAP-F5 and c-CAP-F5 for 30 minutes, as analyzed by flow cytometry. The change in intracellular pH with respect to time as a result of addition of CO₂ in the presence of c-CAP-F5(B) and t-CAP-F5 (C) due to the mechanism shown in (D). The change in intracellular pH of cells incubated with c-CAP-F5 before and after irradiating with 410 nm to isomerize cis isomer to trans isomer (E).

➤ Applied CAP-F5 in an *in vivo* system

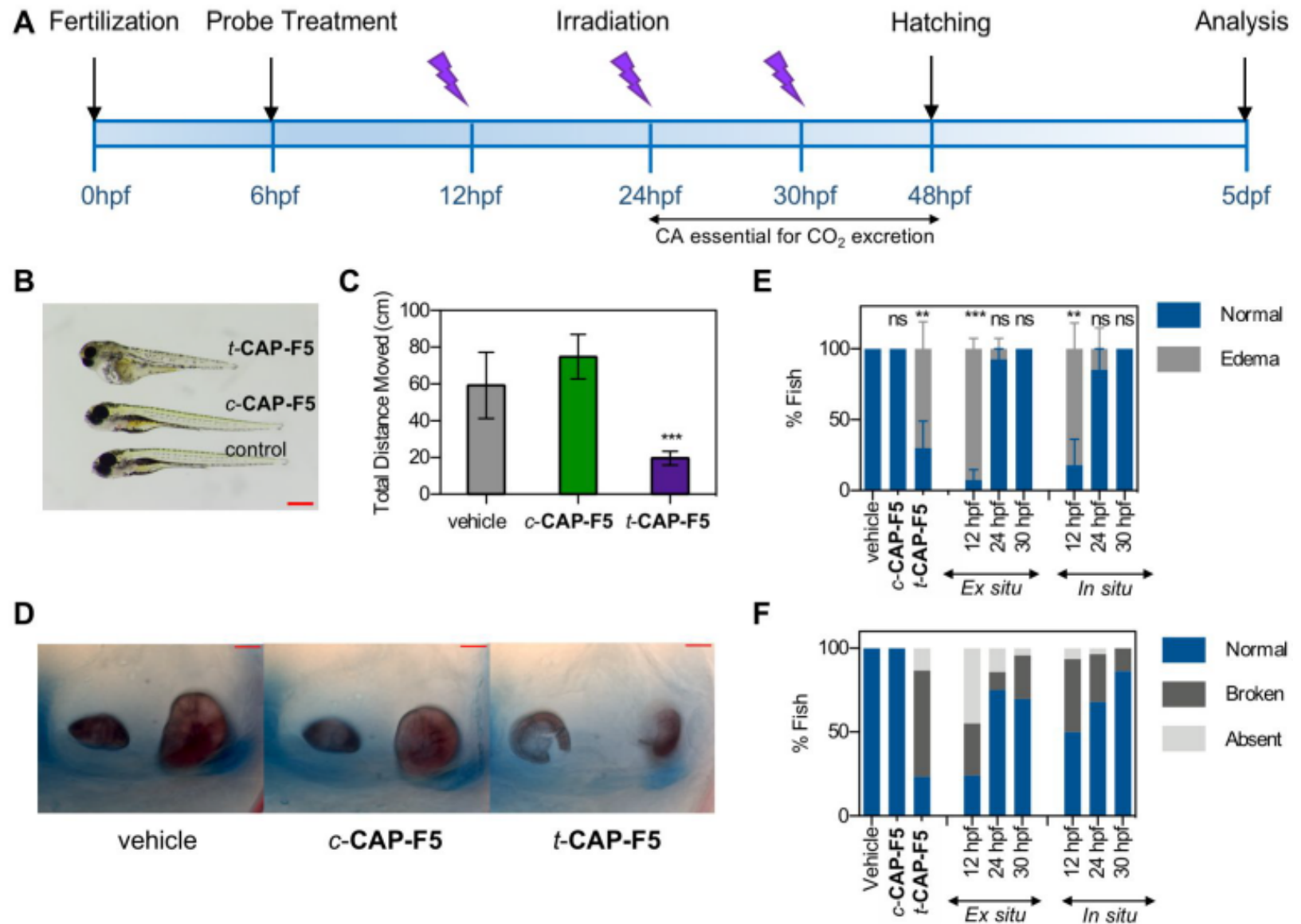


Figure 7. (A) The timeline representing probe treatment and fish analysis. The morphological appearance (B), swimming behavior (C) and otolith development (D) in fish in the absence (vehicle) and presence of t-CAP-F5 and c-CAP-F5. The data represents mean values and the standard deviation. Asterisks denote statistically significant differences ($p < 0.0001$; one-way analysis of variance). Scale bars represents 500 μm and 50 μm for B and D respectively. The morphological (E) and otolith (F) development as a result of in situ activation of probe from cis to trans isomer by irradiating the fish with 410 nm at different time point during embryo development. These developments are compared with ex situ generated trans isomer treatment at the respective time points.